Triplet Excited States of a d^6 Ligand System in a Cubic Field

Tohru Azumi[†,‡] **and Sean P. McGlynn***[,‡]

Akita International University, Yuwa Town, Akita Prefecture, Japan, and Chemistry Department, Louisiana State University, Baton Rouge, Louisiana 70803

Received: February 27, 2004; In Final Form: May 26, 2004

Our concern is the spin sublevels of the first excited triplet state of a d^6 electron system in a cubic field. To that end, we will construct exact analytic eigenvalues and eigenfunctions for these sublevels. The essential point is that we formulate the total wave functions, space plus spin, so that they form bases for the irreducible representations of the O′ double group. By virtue of such a choice, the matrix with respect to the total Hamiltonian, which comprises both crystal field potential and spin−orbit coupling, is a priori diagonalized for any triplet manifold. That is, the symmetry-adapted wave functions are eigenfunctions of the total Hamiltonian. Configuration interaction among the sublevels of different triplet states may also be expressed analytically, and the resulting eigenvalues and eigenfunctions may be obtained as a function of the spin−orbit coupling parameter ς_{nd} and the $^3T_1-{}^3T_2$ energy gap, ΔE (i.e., $8B$, where B is the Racah parameter). The sublevel energies obtained in this way are compared with the energies of the lowest three emitting levels observed for $K_3Co(CN)_6$. From the experimental energy separations, ς_{3d} and B are obtained as 576 and 500 cm^{-1}, respectively. Since these are reasonable values, we conclude that the experimentally identified emitting states are indeed the spin sublevels of the lowest triplet state, $^3T_1$.

1. Introduction

Despite extensive investigation of the luminescence from the lowest triplet state of d^6 ligand field complexes, little is known about the spin sublevels of this state. Since luminescence measurements are usually carried out in the vicinity of 4.2 K, the only emissive sublevel will be the lowest one. Magnetic resonance techniques that have been successful for organic molecules are inapplicable for metal-localized dd transitions for which sublevel splitting is usually in the range 10−100 cm^{-1}: electromagnetic radiation sources in this energy range are not readily available.

The lack of an electromagnetic radiation source to pump the sublevels has been solved ingeniously by Hipps and Crosby[1] who used thermal energy to equilibrate the sublevel populations. They observed a vibrationally structured phosphorescence for $K_3Co(CN)_6$ and identified it as the emission from several of the spin sublevels of the lowest, metal-localized dd triplet state, $^3T_1$. A simulation of the temperature dependence of the phosphorescence lifetimes led to the energies shown in Figure 1. Somewhat later, Mazur and Hipps[2] measured the phosphorescence of various alkali metal complexes of Co(III). The lifetime and quantum yield were found to be highly lattice dependent. However, in all cases, the temperature dependence of the phosphorescence could be fitted satisfactorily by a model in which the observed emission was supposed to be the sum of emissions from three Boltzmann equilibrated sublevels of degeneracies 2, 3, and 3, in agreement with the earlier Hipps/Crosby assignment. In view of the general applicability of a single model to all the lattice-dependent emissions, Mazur and Hipps concluded that the emissive levels were all electronic and most probably associated with the spin sublevels of the $^3T_1$ state of an essentially octahedral complex.

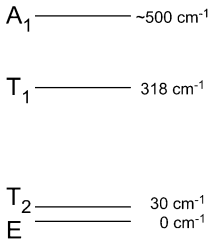

Figure 1. Energies of the spin sublevels associated with the lowest triplet state of $K_3Co(CN)_6$ as determined by Hipps and Crosby.[1] A similar analysis by Mazur and Hipps[2] for a variety of alkali metal complexes of Co(III) found the energies of the second and the third emitting states to be 36 and 315 cm^{-1}, respectively. Since both sets of results are quite similar, we use only the data of ref 1.

The absorption spectra were studied by Miskowski et al.,[3] and on this basis as well as energy considerations, these authors suggested that the emissive triplet state was tetragonally distorted. A Franck−Condon analysis of the vibrationally structured emission by Mazur and Hipps[4] led these authors to favor an octahedral structure although, admittedly, they were unable to rule out a D_{4h} distortion. We will disregard this ambiguity and will assume that the operative field is cubic.

Attempts to locate triplet sublevels by reflectance spectroscopic techniques exist, but they often encounter difficulty. The transitions to the sublevels are certainly spin-forbidden and often spatially forbidden. These difficulties are nicely demonstrated in the reflectance spectra of the heavy-metal complexes reported by Eyring et al.[5] These authors not only identified the triplet sublevels of Rh, Ir, and Pt complexes, they also supported their assignments by extensive large-scale computations. However, the spectra are not very well resolved, leading to errors in peak locations that fall in the range 10−100 cm^{-1} and to the all-too-human inclination to assign an electronic transition to every

* Corresponding author. E-mail: chspm@lsu.edu. Phone: 225-578-3392. Fax: 225-578-2945.
† Akita International University. E-mail: azumi@aiu.ac.jp.
‡ Louisiana State University.

10.1021/jp0491055 CCC: $27.50
Published on Web 07/29/2004

inflection. In any event, it seems impossible to determine sublevel energies to an accuracy of the order of 10 cm^{-1}, which is what Crosby/Hipps obtained and what we have in mind.

As far as we are aware, no theoretical interpretation of the experiments of Hipps and Crosby[1] and of Mazur and Hipps[2] is available. There seems to be no question that the emitting levels are the triplet sublevels; however, further substantiation requires the demonstration that the sublevel energy separations can be interpreted using reasonable magnitudes of the spectroscopic parameters.

To this end, we have developed a theory of the sublevel structure of a system of six d-electrons in a cubic field. We will not engage large calculations; instead, we will demonstrate a process to obtain exact, analytic eigenfunctions and eigenvalues. We are not aware of any such prior efforts for any d^n electron systems.

2. Theory

The notations introduced by Griffith[6] for the five d-orbitals will be used:

$$\xi = d_{yz} = \sqrt{\frac{1}{2}}i(d_1 + d_{-1})$$

$$\eta = d_{zx} = -\sqrt{\frac{1}{2}}(d_1 - d_{-1})$$

$$\varsigma = \sqrt{\frac{1}{2}}i(d_2 - d_{-2})$$

$$\theta = d_{z^2} = d_0$$

$$\epsilon = d_{x^2-y^2} = \sqrt{\frac{1}{2}}(d_2 + d_{-2}) \tag{1}$$

The total Hamiltonian is expressed as

$$H = H_0 + V_C + H_{SO} \tag{2}$$

where H_0 consists of the kinetic energies of electrons and electron−electron repulsions, V_C is the crystal field potential, and H_{SO} is the spin−orbit coupling. H_{SO} is defined as the sum of the one-electron operators:

$$H_{SO} = \sum_i \xi(r) l_i S_i \tag{3}$$

where[7]

$$\xi(r) = \frac{1}{4\pi\epsilon_0}\frac{Ze^2}{2m_e{}^2c^2}\frac{1}{r^3} \tag{4}$$

The triplet excited states arising from the $t_2{}^5e^1$ configurations, as given by the direct product

$$T_2 \times E = T_1 + T_2 \tag{5}$$

are $^3T_1$ and $^3T_2$. When electron repulsions are considered, the energies of these states are

$$\begin{aligned} E(^3T_2) &= 10Dq + 15A - 22B + 12C \\ E(^3T_1) &= 10Dq + 15A - 30B + 12C \end{aligned} \tag{6}$$

where *A*, *B*, and *C* are Racah parameters. Since the parameter *B* is positive, it is immediately clear that $^3T_1$ is the lower triplet state.

TABLE 1: Wave Functions $\psi(^3T_1, M, z)$ and $\psi(^3T_1, \tau, \gamma)$

Table 1a: Wave Functions $\psi(^3T_1, M, z)$[a,b]

$$\psi(^3T_1, M = 1, z) = |\xi\bar{\xi}\eta\bar{\eta}\varsigma\epsilon|$$

$$\psi(^3T_1, M = 0, z) = \frac{1}{\sqrt{2}}\{|\xi\bar{\xi}\eta\bar{\eta}\varsigma\bar{\epsilon}| + |\xi\bar{\xi}\eta\bar{\eta}\bar{\varsigma}\epsilon|\}$$

$$\psi(^3T_1, M = -1, z) = |\xi\bar{\xi}\eta\bar{\eta}\bar{\varsigma}\bar{\epsilon}|$$

Table 1b: Wave Functions $\psi(^3T_1, \tau, \gamma)$[c]

$$\psi(^3T_1, \tau_x, \gamma) = \frac{1}{\sqrt{2}}\{\psi(^3T_1, M = -1, \gamma) - \psi(^3T_1, M = +1, \gamma)\}$$

$$\psi(^3T_1, \tau_y, \gamma) = \frac{1}{\sqrt{2}}i\{\psi(^3T_1, M = -1, \gamma) + \psi(^3T_1, M = +1, \gamma)\}$$

$$\psi(^3T_1, \tau_z, \gamma) = \psi(^3T_1, M = 0, \gamma)$$

[a] The notation $|\xi\bar{\xi}\eta\bar{\eta}\varsigma\epsilon|$ denotes a Slater determinant including the normalization factor of $1/\sqrt{6!}$. [b] The six unlisted *x* and *y* components of the wave functions are obtained from the above by appropriate cyclic interchange of (*x*, *y*, *z*), (ξ, η, ς), and ($-(\sqrt{3}/2)\,\theta - {}^1/_2\epsilon$, $(\sqrt{3}/2)\,\theta - ({}^1/_2)\epsilon$, ϵ). [c] $\gamma = x, y, z$.

We now consider the spin−orbit coupling. The O′ double group representations for which the total wave functions, space plus spin, constitute a basis are given by the direct product of the space representation and the spin representation. Since the triplet spin function transforms as T_1, the $^3T_1$ state yields the sublevels

$$T_1 \times T_1 = A_1 + E + T_1 + T_2 \tag{7}$$

For the higher energy $^3T_2$ state, the direct product

$$T_2 \times T_1 = A_2 + E + T_1 + T_2 \tag{8}$$

also implies a further splitting into four spin sublevels, A_2, E, T_1, and T_2.

The energies of the spin sublevels can be obtained by diagonalizing the matrix of the total Hamiltonian. The procedure is straightforward. However, whether diagonalization can be carried out analytically depends on the choice of the basis functions. Consequently, we intend to construct total wave functions, space plus spin, that are fully symmetry-adapted in the O′ double group. As far as we know, such a procedure has not been carried out previously. Consequently, we may well be a little prolix. However, the advantage is considerable: the Hamiltonian matrix for any sublevel set will be a priori diagonal.

2.1. $^3T_1$ State. In the conventional method, the spatial wave functions are constructed so that they are bases for the irreducible representation T_1 of the single-group O. The spin wave functions are constructed so that they are eigenfunctions of the spin operators S^2 and S_z. These spin functions, as single multipliers, are then used to modify the spatial parts, generating a set of space/spin functions. Finally, the wave functions for the $t_2{}^5e_1$ configuration are then constructed along methods outlined, for example, by Sugano et al.[8] The essence of this method consists of connecting the wave functions of the $t_2{}^5$ and e^1 configurations using the Clebsch−Gordan and Wigner coefficients. Such a set of wave functions is shown in Table 1a. The unique property of these wave functions is that they are not only bases of the irreducible representation T_1 of the O group, but more importantly, each wave function transforms exactly as one of the functions *x*, *y*, or *z*. The wave functions so constructed are labeled *x*, *y*, or *z*.

The wave functions of Table 1a are diagonal with respect to $H_0 + V_C$. The diagonal term is $E(^3T_1)$ of eq 6. If we take $E(^3T_1)$ as the zero of energy, the matrix elements of the total

Hamiltonian, $H_0 + V_C + H_{SO}$, with respect to the nine basis functions are

$$\langle H\rangle = \frac{\varsigma_{nd}}{4\sqrt{2}}\begin{bmatrix} 1x & 1y & 1z & 0x & 0y & 0z & -1x & -1y & -1z \\ 0 & \sqrt{2}i & 0 & 0 & 0 & -1 & 0 & 0 & 0 \\ -\sqrt{2}i & 0 & 0 & 0 & 0 & i & 0 & 0 & 0 \\ 0 & 0 & 0 & 1 & -i & 0 & 0 & 0 & 0 \\ 0 & 0 & 1 & 0 & 0 & 0 & 0 & 0 & 1 \\ 0 & 0 & i & 0 & 0 & 0 & 0 & 0 & i \\ -1 & -i & 0 & 0 & 0 & 0 & -1 & -i & 0 \\ 0 & 0 & 0 & 0 & 0 & -1 & 0 & -\sqrt{2}i & 0 \\ 0 & 0 & 0 & 0 & 0 & i & \sqrt{2}i & 0 & 0 \\ 0 & 0 & 0 & 1 & -i & 0 & 0 & 0 & 0 \end{bmatrix} \tag{9}$$

where ς_{nd}, the spin−orbit coupling parameter[6] for the *nd* state, is

$$\begin{aligned}\varsigma_{nd} &= \hbar^2\langle R_{n2}(r)|\xi(r)|R_{n2}(r)\rangle \\ &= \hbar^2\int_0^\infty R_{n2}(r)\xi(r)R_{n2}(r)r^2\,\mathrm{d}r \\ &= \frac{\hbar^2}{4\pi\epsilon_0}\frac{Ze^2}{2m_e{}^2c^2}\int_0^\infty R_{n2}(r)\frac{1}{r^3}R_{n2}(r)r^2\,\mathrm{d}r\end{aligned} \tag{10}$$

This matrix is not diagonal because the functions of Table 1a are not symmetry-adapted in the O′ double group. The diagonalization of this matrix can be carried out numerically; however, diagonalization in an analytical form appears difficult, if not impossible. This is unsatisfactory because it evades full utilization of group theory. If the group theory is properly applied, this nine-dimensional matrix will be a priori blocked into one one-dimensional matrix (A_1), one two-dimensional matrix (E), and two three-dimensional matrices (T_1 and T_2).

The crucial point of the basis functions shown in Table 1a is that even though they are bases of irreducible representations of the O single group, they are not bases for irreducible representations of the O′ double group. The crux lies in a choice of spin functions that are symmetry-adapted in O′. Indeed, since no external magnetic field is applied, there is little physical sense in choosing spin functions to be eigenfunctions of S_z.

Consider the following linear combinations of the spin functions:

$$\begin{aligned}\tau_x &= \frac{1}{\sqrt{2}}\{\psi(M=-1) - \psi(M=+1)\} \\ \tau_y &= \frac{1}{\sqrt{2}}i\{\psi(M=-1) + \psi(M=+1)\} \\ \tau_z &= \psi(M=0)\end{aligned} \tag{11}$$

These spin functions constitute a basis for the T_1 irreducible representation of O′. Furthermore, τ_x, τ_y, and τ_z transform in the same way as the functions x, y, and z, respectively, in the O′ double group. In view of this property, we take the linear combinations of Table 1b to be the new basis set of spin functions.

If the group operations of O′ are applied to the space parts of the wave functions of Table 1b, it is found that they transform as the irreducible representation T_1. Likewise, if the same operations are applied to the spin parts, it is found that these also transform as the irreducible representation T_1. However, if the O′ symmetry operations are applied simultaneously to both space and spin parts, it is found that none of these wave functions constitute bases for any irreducible representation of O′. However, since both the space part and spin part of each wave function transform identically to some one of the functions, x, y, z, these parts may be combined using the Clebsch−Gordan coefficients to yield wave functions that are bases for irreducible representations of O′. The final basis set of wave functions chosen in this way is summarized in Table 2 and, when expressed in terms of Slater determinants, in Table 3.

TABLE 2: Wave Functions of the Spin Sublevels $\psi(^3T_1, \Gamma, \gamma)$ that Are Bases for Irreducible Representations of the Point Group O′

$$\psi(^3T_1, A_1, e_1) = -\frac{1}{\sqrt{3}}\psi(^3T_1, \tau_x, x) - \frac{1}{\sqrt{3}}\psi(^3T_1, \tau_y, y) - \frac{1}{\sqrt{3}}\psi(^3T_1, \tau_z, z)$$

$$\psi(^3T_1, E, \theta) = \frac{1}{\sqrt{6}}\psi(^3T_1, \tau_x, x) + \frac{1}{\sqrt{6}}\psi(^3T_1, \tau_y, y) - \frac{2}{\sqrt{6}}\psi(^3T_1, \tau_z, z)$$

$$\psi(^3T_1, E, \epsilon) = -\frac{1}{\sqrt{2}}\psi(^3T_1, \tau_x, x) + \frac{1}{\sqrt{2}}\psi(^3T_1, \tau_y, y)$$

$$\psi(^3T_1, T_1, x) = -\frac{1}{\sqrt{2}}\psi(^3T_1, \tau_y, z) + \frac{1}{\sqrt{2}}\psi(^3T_1, \tau_z, y)$$

$$\psi(^3T_1, T_1, y) = \frac{1}{\sqrt{2}}\psi(^3T_1, \tau_x, z) - \frac{1}{\sqrt{2}}\psi(^3T_1, \tau_z, x)$$

$$\psi(^3T_1, T_1, z) = -\frac{1}{\sqrt{2}}\psi(^3T_1, \tau_x, y) + \frac{1}{\sqrt{2}}\psi(^3T_1, \tau_y, x)$$

$$\psi(^3T_1, T_2, \xi) = -\frac{1}{\sqrt{2}}\psi(^3T_1, \tau_y, z) - \frac{1}{\sqrt{2}}\psi(^3T_1, \tau_z, y)$$

$$\psi(^3T_1, T_2, \eta) = -\frac{1}{\sqrt{2}}\psi(^3T_1, \tau_x, z) - \frac{1}{\sqrt{2}}\psi(^3T_1, \tau_z, x)$$

$$\psi(^3T_1, T_2, \varsigma) = -\frac{1}{\sqrt{2}}\psi(^3T_1, \tau_x, y) - \frac{1}{\sqrt{2}}\psi(^3T_1, \tau_y, x)$$

The Hamiltonian matrix based on these functions is given in Table 4. As shown in Table 4, the nine-dimensional matrix is not only blocked out into one one-dimensional, one two-dimensional, and two three-dimensional matrices, it is also completely diagonal. This property is a result of the mode of construction: each component transforms as either one of the d-orbitals (ξ, η, ς, θ, or ϵ) or one of p-orbitals (x, y, or z).

2.2. $^3T_2$ State. Similar procedures may be applied to the second excited triplet state, $^3T_2$. The Hamiltonian matrix based on basis functions that were constructed so that only the space part is a basis for the irreducible representation T_2 is

$$\langle H\rangle = \frac{\varsigma_{nd}}{4\sqrt{2}}\times \begin{bmatrix} 1\xi & 1\eta & 1\varsigma & 0\xi & 0\eta & 0\varsigma & -1\xi & -1\eta & -1\varsigma \\ 0 & \sqrt{2}i & 0 & 0 & 0 & -1 & 0 & 0 & 0 \\ -\sqrt{2}i & 0 & 0 & 0 & 0 & i & 0 & 0 & 0 \\ 0 & 0 & 0 & 1 & -i & 0 & 0 & 0 & 0 \\ 0 & 0 & 1 & 0 & 0 & 0 & 0 & 0 & -1 \\ 0 & 0 & i & 0 & 0 & 0 & 0 & 0 & i \\ -1 & -i & 0 & 0 & 0 & 0 & 1 & i & 0 \\ 0 & 0 & 0 & 0 & 0 & 1 & 0 & -\sqrt{2}i & 0 \\ 0 & 0 & 0 & 0 & 0 & -i & \sqrt{2}i & 0 & 0 \\ 0 & 0 & 0 & -1 & -i & 0 & 0 & 0 & 0 \end{bmatrix} \tag{12}$$

TABLE 3: Wave Functions of the Spin Sublevels $\psi(^3T_1, \Gamma, \gamma)$ that Are Bases for Irreducible Representations of the Point Group O′

$$\psi(^3T_1, A_1, e_1) = -\frac{1}{2\sqrt{2}}|\xi\eta\bar{\eta}\varsigma\bar{\varsigma}\theta| + \frac{1}{2\sqrt{2}}|\bar{\xi}\eta\bar{\eta}\varsigma\bar{\varsigma}\bar{\theta}| - \frac{1}{2\sqrt{6}}|\xi\eta\bar{\eta}\varsigma\bar{\varsigma}\epsilon| + \frac{1}{2\sqrt{6}}|\bar{\xi}\eta\bar{\eta}\varsigma\bar{\varsigma}\bar{\epsilon}| - \frac{1}{2\sqrt{2}}i|\xi\bar{\xi}\eta\varsigma\bar{\varsigma}\theta| - \frac{1}{2\sqrt{2}}i|\xi\bar{\xi}\bar{\eta}\varsigma\bar{\varsigma}\bar{\theta}| + \frac{1}{2\sqrt{6}}i|\xi\bar{\xi}\eta\varsigma\bar{\varsigma}\epsilon| + \frac{1}{2\sqrt{6}}i|\xi\bar{\xi}\bar{\eta}\varsigma\bar{\varsigma}\bar{\epsilon}| - \frac{1}{\sqrt{6}}|\xi\bar{\xi}\eta\bar{\eta}\varsigma\bar{\epsilon}| - \frac{1}{\sqrt{6}}|\xi\bar{\xi}\eta\bar{\eta}\bar{\varsigma}\epsilon|$$

$$\psi(^3T_1, E, \theta) = \frac{1}{4}|\xi\eta\bar{\eta}\varsigma\bar{\varsigma}\theta| - \frac{1}{4}|\bar{\xi}\eta\bar{\eta}\varsigma\bar{\varsigma}\bar{\theta}| + \frac{1}{4\sqrt{3}}|\xi\eta\bar{\eta}\varsigma\bar{\varsigma}\epsilon| - \frac{1}{4\sqrt{3}}|\bar{\xi}\eta\bar{\eta}\varsigma\bar{\varsigma}\bar{\epsilon}| + \frac{1}{4}i|\xi\bar{\xi}\eta\varsigma\bar{\varsigma}\theta| + \frac{1}{4}i|\xi\bar{\xi}\bar{\eta}\varsigma\bar{\varsigma}\bar{\theta}| - \frac{1}{4\sqrt{3}}i|\xi\bar{\xi}\eta\varsigma\bar{\varsigma}\epsilon| - \frac{1}{4\sqrt{3}}i|\xi\bar{\xi}\bar{\eta}\varsigma\bar{\varsigma}\bar{\epsilon}| - \frac{1}{\sqrt{3}}|\xi\bar{\xi}\eta\bar{\eta}\varsigma\bar{\epsilon}| - \frac{1}{\sqrt{3}}|\xi\bar{\xi}\eta\bar{\eta}\bar{\varsigma}\epsilon|$$

$$\psi(^3T_1, E, \epsilon) = -\frac{\sqrt{3}}{4}|\xi\eta\bar{\eta}\varsigma\bar{\varsigma}\theta| + \frac{\sqrt{3}}{4}|\bar{\xi}\eta\bar{\eta}\varsigma\bar{\varsigma}\bar{\theta}| - \frac{1}{4}|\xi\eta\bar{\eta}\varsigma\bar{\varsigma}\epsilon| + \frac{1}{4}|\bar{\xi}\eta\bar{\eta}\varsigma\bar{\varsigma}\bar{\epsilon}| + \frac{\sqrt{3}}{4}i|\xi\bar{\xi}\eta\varsigma\bar{\varsigma}\theta| + \frac{\sqrt{3}}{4}i|\xi\bar{\xi}\bar{\eta}\varsigma\bar{\varsigma}\bar{\theta}| - \frac{1}{4}i|\xi\bar{\xi}\eta\varsigma\bar{\varsigma}\epsilon| - \frac{1}{4}i|\xi\bar{\xi}\bar{\eta}\varsigma\bar{\varsigma}\bar{\epsilon}|$$

$$\psi(^3T_1, T_1, x) = \frac{\sqrt{3}}{4}|\xi\bar{\xi}\eta\varsigma\bar{\varsigma}\bar{\theta}| + \frac{\sqrt{3}}{4}|\xi\bar{\xi}\bar{\eta}\varsigma\bar{\varsigma}\theta| - \frac{1}{4}|\xi\bar{\xi}\eta\varsigma\bar{\varsigma}\bar{\epsilon}| - \frac{1}{4}|\xi\bar{\xi}\bar{\eta}\varsigma\bar{\varsigma}\epsilon| - \frac{1}{2}i|\xi\bar{\xi}\eta\bar{\eta}\varsigma\epsilon| - \frac{1}{2}i|\xi\bar{\xi}\eta\bar{\eta}\bar{\varsigma}\bar{\epsilon}|$$

$$\psi(^3T_1, T_1, y) = \frac{\sqrt{3}}{4}|\xi\eta\bar{\eta}\varsigma\bar{\varsigma}\bar{\theta}| + \frac{\sqrt{3}}{4}|\bar{\xi}\eta\bar{\eta}\varsigma\bar{\varsigma}\theta| + \frac{1}{4}|\xi\eta\bar{\eta}\varsigma\bar{\varsigma}\bar{\epsilon}| + \frac{1}{4}|\bar{\xi}\eta\bar{\eta}\varsigma\bar{\varsigma}\epsilon| - \frac{1}{2}|\xi\bar{\xi}\eta\bar{\eta}\varsigma\epsilon| + \frac{1}{2}|\xi\bar{\xi}\eta\bar{\eta}\bar{\varsigma}\bar{\epsilon}|$$

$$\psi(^3T_1, T_1, z) = -\frac{\sqrt{3}}{4}i|\xi\eta\bar{\eta}\varsigma\bar{\varsigma}\theta| - \frac{\sqrt{3}}{4}i|\bar{\xi}\eta\bar{\eta}\varsigma\bar{\varsigma}\bar{\theta}| - \frac{1}{4}i|\xi\eta\bar{\eta}\varsigma\bar{\varsigma}\epsilon| - \frac{1}{4}i|\bar{\xi}\eta\bar{\eta}\varsigma\bar{\varsigma}\bar{\epsilon}| + \frac{\sqrt{3}}{4}|\xi\bar{\xi}\eta\varsigma\bar{\varsigma}\theta| - \frac{\sqrt{3}}{4}|\xi\bar{\xi}\bar{\eta}\varsigma\bar{\varsigma}\bar{\theta}| - \frac{1}{4}|\xi\bar{\xi}\eta\varsigma\bar{\varsigma}\epsilon| + \frac{1}{4}|\xi\bar{\xi}\bar{\eta}\varsigma\bar{\varsigma}\bar{\epsilon}|$$

$$\psi(^3T_1, T_2, \xi) = -\frac{\sqrt{3}}{4}|\xi\bar{\xi}\eta\varsigma\bar{\varsigma}\bar{\theta}| - \frac{\sqrt{3}}{4}|\xi\bar{\xi}\bar{\eta}\varsigma\bar{\varsigma}\theta| + \frac{1}{4}|\xi\bar{\xi}\eta\varsigma\bar{\varsigma}\bar{\epsilon}| + \frac{1}{4}|\xi\bar{\xi}\bar{\eta}\varsigma\bar{\varsigma}\epsilon| - \frac{1}{2}i|\xi\bar{\xi}\eta\bar{\eta}\varsigma\epsilon| - \frac{1}{2}i|\xi\bar{\xi}\eta\bar{\eta}\bar{\varsigma}\bar{\epsilon}|$$

$$\psi(^3T_1, T_2, \eta) = \frac{\sqrt{3}}{4}|\xi\eta\bar{\eta}\varsigma\bar{\varsigma}\bar{\theta}| + \frac{\sqrt{3}}{4}|\bar{\xi}\eta\bar{\eta}\varsigma\bar{\varsigma}\theta| + \frac{1}{4}|\xi\eta\bar{\eta}\varsigma\bar{\varsigma}\bar{\epsilon}| + \frac{1}{4}|\bar{\xi}\eta\bar{\eta}\varsigma\bar{\varsigma}\epsilon| + \frac{1}{2}|\xi\bar{\xi}\eta\bar{\eta}\varsigma\epsilon| - \frac{1}{2}|\xi\bar{\xi}\eta\bar{\eta}\bar{\varsigma}\bar{\epsilon}|$$

$$\psi(^3T_1, T_2, \varsigma) = \frac{\sqrt{3}}{4}i|\xi\eta\bar{\eta}\varsigma\bar{\varsigma}\theta| + \frac{\sqrt{3}}{4}i|\bar{\xi}\eta\bar{\eta}\varsigma\bar{\varsigma}\bar{\theta}| + \frac{1}{4}i|\xi\eta\bar{\eta}\varsigma\bar{\varsigma}\epsilon| + \frac{1}{4}i|\bar{\xi}\eta\bar{\eta}\varsigma\bar{\varsigma}\bar{\epsilon}| + \frac{\sqrt{3}}{4}|\xi\bar{\xi}\eta\varsigma\bar{\varsigma}\theta| - \frac{\sqrt{3}}{4}|\xi\bar{\xi}\bar{\eta}\varsigma\bar{\varsigma}\bar{\theta}| - \frac{1}{4}|\xi\bar{\xi}\eta\varsigma\bar{\varsigma}\epsilon| + \frac{1}{4}|\xi\bar{\xi}\bar{\eta}\varsigma\bar{\varsigma}\bar{\epsilon}|$$

TABLE 4: Hamiltonian Matrix Elements with Respect to the Basis Functions $\psi(^3T_1, \Gamma, \gamma)$

	A_1, e_1	E, θ	E, ϵ	T_1, x	T_1, y	T_1, z	T_2, ξ	T_2, η	T_2, ς
A_1, e_1	$E(^3T_1) + \frac{1}{2}\varsigma_{nd}$	0	0	0	0	0	0	0	0
E, θ	0	$E(^3T_1) - \frac{1}{4}\varsigma_{nd}$	0	0	0	0	0	0	0
E, ϵ	0	0	$E(^3T_1) - \frac{1}{4}\varsigma_{nd}$	0	0	0	0	0	0
T_1, x	0	0	0	$E(^3T_1) + \frac{1}{4}\varsigma_{nd}$	0	0	0	0	0
T_1, y	0	0	0	0	$E(^3T_1) + \frac{1}{4}\varsigma_{nd}$	0	0	0	0
T_1, z	0	0	0	0	0	$E(^3T_1) + \frac{1}{4}\varsigma_{nd}$	0	0	0
T_2, ξ	0	0	0	0	0	0	$E(^3T_1) - \frac{1}{4}\varsigma_{nd}$	0	0
T_2, η	0	0	0	0	0	0	0	$E(^3T_1) - \frac{1}{4}\varsigma_{nd}$	0
T_2, ς	0	0	0	0	0	0	0	0	$E(^3T_1) - \frac{1}{4}\varsigma_{nd}$

where the zero of energy is defined as $E(^3T_2)$. This matrix is difficult to diagonalize analytically.

The wave functions that are bases for the irreducible representations $^3T_2$ of the O′ double group can be constructed in a manner that is identical to that for $^3T_1$. These wave functions are shown in Table 5. The Hamiltonian matrix based on the wave functions of Table 5 is shown in Table 6. This matrix is also a priori diagonal.

2.3. Configuration Interaction Between $^3T_1$ Sublevels and $^3T_2$ Sublevels. The wave functions and energies of Tables 3, 4, 5, and 6 are exact eigenfunctions and eigenvalues of the total Hamiltonian provided that configuration interaction between $^3T_1$

TABLE 5: Wavefunctions of the Spin Sublevels $\psi(^3T_2, \Gamma, \gamma)$ that Are Bases for Irreducible Representations of the Point Group O′

$$\psi(^3T_2, A_2, e_2) = -\frac{1}{2\sqrt{6}}|\xi\eta\bar{\eta}\varsigma\bar{\varsigma}\theta| + \frac{1}{2\sqrt{6}}|\bar{\xi}\eta\bar{\eta}\varsigma\bar{\varsigma}\bar{\theta}| + \frac{1}{2\sqrt{2}}|\xi\eta\bar{\eta}\varsigma\bar{\varsigma}\epsilon| - \frac{1}{2\sqrt{2}}|\bar{\xi}\eta\bar{\eta}\varsigma\bar{\varsigma}\bar{\epsilon}| + \frac{1}{2\sqrt{6}}i|\xi\bar{\xi}\eta\varsigma\bar{\varsigma}\bar{\theta}| + \frac{1}{2\sqrt{6}}i|\xi\bar{\xi}\bar{\eta}\varsigma\bar{\varsigma}\bar{\theta}| + \frac{1}{2\sqrt{2}}i|\xi\bar{\xi}\eta\varsigma\bar{\varsigma}\epsilon| + \frac{1}{2\sqrt{2}}i|\xi\bar{\xi}\bar{\eta}\varsigma\bar{\varsigma}\bar{\epsilon}| - \frac{1}{\sqrt{6}}|\xi\bar{\xi}\eta\bar{\eta}\varsigma\bar{\theta}| - \frac{1}{\sqrt{6}}|\xi\bar{\xi}\eta\bar{\eta}\bar{\varsigma}\theta|$$

$$\psi(^3T_2, E, \theta) = -\frac{1}{4}|\xi\eta\bar{\eta}\varsigma\bar{\varsigma}\theta| + \frac{1}{4}|\bar{\xi}\eta\bar{\eta}\varsigma\bar{\varsigma}\bar{\theta}| + \frac{\sqrt{3}}{4}|\xi\eta\bar{\eta}\varsigma\bar{\varsigma}\epsilon| - \frac{\sqrt{3}}{4}|\bar{\xi}\eta\bar{\eta}\varsigma\bar{\varsigma}\bar{\epsilon}| - \frac{1}{4}i|\xi\bar{\xi}\eta\varsigma\bar{\varsigma}\theta| - \frac{1}{4}i|\xi\bar{\xi}\bar{\eta}\varsigma\bar{\varsigma}\bar{\theta}| - \frac{\sqrt{3}}{4}i|\xi\bar{\xi}\eta\varsigma\bar{\varsigma}\epsilon| - \frac{\sqrt{3}}{4}i|\xi\bar{\xi}\bar{\eta}\varsigma\bar{\varsigma}\bar{\epsilon}|$$

$$\psi(^3T_2, E, \epsilon) = -\frac{1}{4\sqrt{3}}|\xi\eta\bar{\eta}\varsigma\bar{\varsigma}\theta| + \frac{1}{4\sqrt{3}}|\bar{\xi}\eta\bar{\eta}\varsigma\bar{\varsigma}\bar{\theta}| + \frac{1}{4}|\xi\eta\bar{\eta}\varsigma\bar{\varsigma}\epsilon| - \frac{1}{4}|\bar{\xi}\eta\bar{\eta}\varsigma\bar{\varsigma}\bar{\epsilon}| + \frac{1}{4\sqrt{3}}i|\xi\bar{\xi}\eta\varsigma\bar{\varsigma}\theta| + \frac{1}{4\sqrt{3}}i|\xi\bar{\xi}\bar{\eta}\varsigma\bar{\varsigma}\bar{\theta}| + \frac{1}{4}i|\xi\bar{\xi}\eta\varsigma\bar{\varsigma}\epsilon| + \frac{1}{4}i|\xi\bar{\xi}\bar{\eta}\varsigma\bar{\varsigma}\bar{\epsilon}| + \frac{1}{\sqrt{3}}|\xi\bar{\xi}\eta\bar{\eta}\varsigma\bar{\theta}| + \frac{1}{\sqrt{3}}|\xi\bar{\xi}\eta\bar{\eta}\bar{\varsigma}\theta|$$

$$\psi(^3T_2, T_1, x) = -\frac{1}{4}|\xi\bar{\xi}\eta\varsigma\bar{\varsigma}\bar{\theta}| - \frac{1}{4}|\xi\bar{\xi}\bar{\eta}\varsigma\bar{\varsigma}\theta| - \frac{\sqrt{3}}{4}|\xi\bar{\xi}\eta\varsigma\bar{\varsigma}\bar{\epsilon}| - \frac{\sqrt{3}}{4}|\xi\bar{\xi}\bar{\eta}\varsigma\bar{\varsigma}\epsilon| + \frac{1}{2}i|\bar{\xi}\xi\eta\bar{\eta}\varsigma\theta| + \frac{1}{2}i|\xi\bar{\xi}\eta\bar{\eta}\bar{\varsigma}\bar{\theta}|$$

$$\psi(^3T_2, T_1, y) = -\frac{1}{4}|\xi\eta\bar{\eta}\varsigma\bar{\varsigma}\bar{\theta}| - \frac{1}{4}|\bar{\xi}\eta\bar{\eta}\varsigma\bar{\varsigma}\theta| + \frac{\sqrt{3}}{4}|\xi\eta\bar{\eta}\varsigma\bar{\varsigma}\bar{\epsilon}| + \frac{\sqrt{3}}{4}|\bar{\xi}\eta\bar{\eta}\varsigma\bar{\varsigma}\epsilon| - \frac{1}{2}|\xi\bar{\xi}\eta\bar{\eta}\varsigma\theta| + \frac{1}{2}|\xi\bar{\xi}\eta\bar{\eta}\bar{\varsigma}\bar{\theta}|$$

$$\psi(^3T_2, T_1, z) = -\frac{1}{4}i|\xi\eta\bar{\eta}\varsigma\bar{\varsigma}\theta| - \frac{1}{4}i|\bar{\xi}\eta\bar{\eta}\varsigma\bar{\varsigma}\bar{\theta}| + \frac{\sqrt{3}}{4}i|\xi\eta\bar{\eta}\varsigma\bar{\varsigma}\epsilon| + \frac{\sqrt{3}}{4}i|\bar{\xi}\eta\bar{\eta}\varsigma\bar{\varsigma}\bar{\epsilon}| + \frac{1}{4}|\xi\bar{\xi}\eta\varsigma\bar{\varsigma}\theta| - \frac{1}{4}|\xi\bar{\xi}\bar{\eta}\varsigma\bar{\varsigma}\bar{\theta}| + \frac{\sqrt{3}}{4}|\xi\bar{\xi}\eta\varsigma\bar{\varsigma}\epsilon| - \frac{\sqrt{3}}{4}|\xi\bar{\xi}\bar{\eta}\varsigma\bar{\varsigma}\bar{\epsilon}|$$

$$\psi(^3T_2, T_2, \xi) = -\frac{1}{4}|\xi\bar{\xi}\eta\varsigma\bar{\varsigma}\bar{\theta}| - \frac{1}{4}|\xi\bar{\xi}\bar{\eta}\varsigma\bar{\varsigma}\theta| - \frac{\sqrt{3}}{4}|\xi\bar{\xi}\eta\varsigma\bar{\varsigma}\bar{\epsilon}| - \frac{\sqrt{3}}{4}|\xi\bar{\xi}\bar{\eta}\varsigma\bar{\varsigma}\epsilon| - \frac{1}{2}i|\xi\bar{\xi}\eta\bar{\eta}\varsigma\theta| - \frac{1}{2}i|\xi\bar{\xi}\eta\bar{\eta}\bar{\varsigma}\bar{\theta}|$$

$$\psi(^3T_2, T_2, \eta) = \frac{1}{4}|\xi\eta\bar{\eta}\varsigma\bar{\varsigma}\bar{\theta}| + \frac{1}{4}|\bar{\xi}\eta\bar{\eta}\varsigma\bar{\varsigma}\theta| - \frac{\sqrt{3}}{4}|\xi\eta\bar{\eta}\varsigma\bar{\varsigma}\bar{\epsilon}| - \frac{\sqrt{3}}{4}|\bar{\xi}\eta\bar{\eta}\varsigma\bar{\varsigma}\epsilon| - \frac{1}{2}|\xi\bar{\xi}\eta\bar{\eta}\varsigma\theta| + \frac{1}{2}|\xi\bar{\xi}\eta\bar{\eta}\bar{\varsigma}\bar{\theta}|$$

$$\psi(^3T_2, T_2, \varsigma) = -\frac{1}{4}i|\xi\eta\bar{\eta}\varsigma\bar{\varsigma}\theta| - \frac{1}{4}i|\bar{\xi}\eta\bar{\eta}\varsigma\bar{\varsigma}\bar{\theta}| + \frac{\sqrt{3}}{4}i|\xi\eta\bar{\eta}\varsigma\bar{\varsigma}\epsilon| + \frac{\sqrt{3}}{4}i|\bar{\xi}\eta\bar{\eta}\varsigma\bar{\varsigma}\bar{\epsilon}| - \frac{1}{4}|\xi\bar{\xi}\eta\varsigma\bar{\varsigma}\theta| + \frac{1}{4}|\xi\bar{\xi}\bar{\eta}\varsigma\bar{\varsigma}\bar{\theta}| - \frac{\sqrt{3}}{4}|\xi\bar{\xi}\eta\varsigma\bar{\varsigma}\epsilon| + \frac{\sqrt{3}}{4}|\xi\bar{\xi}\bar{\eta}\varsigma\bar{\varsigma}\bar{\epsilon}|$$

TABLE 6: Hamiltonian Matrix Elements with Respect to the Wavefunctions $\psi(^3T_2, \Gamma, \gamma)$

	A_2, e_2	E, θ	E, ϵ	T_1, x	T_1, y	T_1, z	T_2, ξ	T_2, η	T_2, ς
A_2, e_2	$E(^3T_2) + \frac{1}{2}\varsigma_{nd}$	0	0	0	0	0	0	0	0
E, θ	0	$E(^3T_2) - \frac{1}{4}\varsigma_{nd}$	0	0	0	0	0	0	0
E, ϵ	0	0	$E(^3T_2) - \frac{1}{4}\varsigma_{nd}$	0	0	0	0	0	0
T_1, x	0	0	0	$E(^3T_2) - \frac{1}{4}\varsigma_{nd}$	0	0	0	0	0
T_1, y	0	0	0	0	$E(^3T_2) - \frac{1}{4}\varsigma_{nd}$	0	0	0	0
T_1, z	0	0	0	0	0	$E(^3T_2) - \frac{1}{4}\varsigma_{nd}$	0	0	0
T_2, ξ	0	0	0	0	0	0	$E(^3T_2) + \frac{1}{4}\varsigma_{nd}$	0	0
T_2, η	0	0	0	0	0	0	0	$E(^3T_2) + \frac{1}{4}\varsigma_{nd}$	0
T_2, ς	0	0	0	0	0	0	0	0	$E(^3T_2) + \frac{1}{4}\varsigma_{nd}$

and $^3T_2$ is neglected. However, if the $^3T_1-{}^3T_2$ energy separation is small, configuration interaction may become significant. Nonetheless, since interaction between these two states by either electron repulsion or the crystal field potential is zero, we need only focus on the spin−orbit coupling.

It is particularly important to direct attention to the two lowest sublevels associated with the lowest triplet state, $^3T_1$. As is shown in Table 4, two of these sublevels, E and T_2, are accidentally degenerate. Thus, it is of some interest to find out if spin−orbit interactions removes this degeneracy. The con-

TABLE 7: Matrix Elements for Configuration Interactions

(1) E Representation, $\gamma = \theta, \epsilon$		
	$\psi(^3T_1, E, \gamma)$	$\psi(^3T_1, E, \gamma)$
$\psi(^3T_1, E, \gamma)$	$E(^3T_1) - \frac{1}{4}\varsigma_{nd}$	$-\frac{3}{4}\varsigma_{nd}$
$\psi(^3T_2, E, \gamma)$	$-\frac{3}{4}\varsigma_{nd}$	$E(^3T_2) - \frac{1}{4}\varsigma_{nd}$
(2) T_2 Representation, $\gamma = \xi, \eta, \varsigma$		
	$\psi(^3T_1, T_2, \gamma)$	$\psi(^3T_2, T_2, \gamma)$
$\psi(^3T_1, T_2, \gamma)$	$E(^3T_1) - \frac{1}{4}\varsigma_{nd}$	$\frac{\sqrt{3}}{4}\varsigma_{nd}$
$\psi(^3T_2, T_2, \gamma)$	$\frac{\sqrt{3}}{4}\varsigma_{nd}$	$E(^3T_2) - \frac{1}{4}\varsigma_{nd}$
(3) T_1 Representation, $\gamma = x, y, z$		
	$\psi(^3T_1, T_1, \gamma)$	$\psi(^3T_2, T_1, \gamma)$
$\psi(^3T_1, T_1, \gamma)$	$E(^3T_1) + \frac{1}{4}\varsigma_{nd}$	$\frac{\sqrt{3}}{4}\varsigma_{nd}$
$\psi(^3T_2, T_1, \gamma)$	$\frac{\sqrt{3}}{4}\varsigma_{nd}$	$E(^3T_2) + \frac{1}{4}\varsigma_{nd}$

figuration interaction matrix elements for the E, T_2, and T_1 states based on the wave functions of Tables 3 and 5 are shown in Table 7. Since all the matrices are two-dimensional, the energies can be solved analytically. They are as follows:

$$E'_{\pm}(E) = E(^3T_1) - \frac{1}{4}\varsigma_{nd} + \frac{1}{2}\Delta E \pm \frac{1}{2}\Delta E\sqrt{1 + \frac{9}{4}\left(\frac{\varsigma_{nd}}{\Delta E}\right)^2} \quad (13)$$

$$E'_{\pm}(T_2) = E(^3T_1) - \frac{1}{4}\varsigma_{nd} + \frac{\Delta E + \varsigma_{nd}/2}{2} \pm \frac{\Delta E + \varsigma_{nd}/2}{2}\sqrt{1 + \frac{3}{4}\left(\frac{\varsigma_{nd}}{\Delta E + \varsigma_{nd}/2}\right)^2} \quad (14)$$

$$E'_{\pm}(T_1) = E(^3T_1) + \frac{1}{4}\varsigma_{nd} + \frac{\Delta E - \varsigma_{nd}/2}{2} \pm \frac{\Delta E - \varsigma_{nd}/2}{2}\sqrt{1 + \frac{3}{4}\left(\frac{\varsigma_{nd}}{\Delta E - \varsigma_{nd}/2}\right)^2} \quad (15)$$

where

$$\Delta E = E(^3T_2) - E(^3T_1) \quad (16)$$

These results are exact; however, approximate energies in the limit of large ΔE may be obtained by expanding the square root. The approximate energies obtained in this limit are indicated in the schematic diagram shown in Figure 2.

3. Comparison with Experiment

We are now ready to compare theory with the experimental results of Hipps and Crosby.[1] First, the assignments and energetic ordering of the sublevels cited by Hipps and Crosby[1] are shown in Figure 1 and are congruent with the theoretical results of Figure 2. Second, the small splitting of the two lowest lying sublevels, T_2 and E, is in accord with prediction. In view of this qualitative agreement we now become more quantitative. If the energy separation between the second (T_2) and third (T_1) sublevels and the energy separation between the lowest two

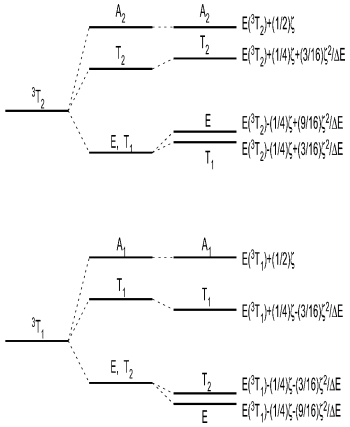

Figure 2. Schematic representation of the theoretically determined energies of the spin sublevels associated with the two triplet excited states of a system of six d-electrons in a cubic field. Left: spin−orbit coupling is not considered. Center: spin−orbit coupling is considered to first order. Right: spin−orbit coupling is fully considered. $E(^3T_2)$ and $E(^3T_2)$ are defined in eq 6; ς is the spin−orbit coupling parameter, ς_{nd}, defined in eq 10 of the text; ΔE is defined in eq 16. The energies shown in the figure are approximate values obtained in the limit of large ΔE. The exact energies are given in the text.

sublevels (E and T_2) are equated to the experimental results, we find

$$\frac{1}{2}\varsigma_{nd} = 288\ \text{cm}^{-1}; \quad \frac{3}{8}\frac{\varsigma_{nd}^2}{8B} = 30\ \text{cm}^{-1} \quad (17)$$

which yields

$$\varsigma_{3d} = 586\ \text{cm}^{-1}; \quad B = 518\ \text{cm}^{-1} \quad (18)$$

The ς_{3d} and B parameters for the neutral Co atom given by Griffith[6] are 517 and 798 cm^{-1}, respectively, and are fairly close to the magnitudes obtained above for Co(III). In view of this comparison, we can say that the spectroscopic parameters obtained on the basis of comparison of theory with the Hipps/Crosby experiments are quite reasonable.

Pierloot et al.[9] have calculated the $^3T_1-^3T_2$ energy gap by a variety of computational quantum approaches. In all instances, this gap turned out to be about 0.5 eV. Since the magnitude of this gap is also $8B$, one finds B to be approximately 500 cm^{-1}, in good accord with the value of 518 cm^{-1} obtained here.

We have no theoretical basis to judge which triplet state geometry, that of Hipps and Crosby[1] or Miskowski et al.[3] is the more trustworthy. However, we can state that the existing assignments do not contradict theory with regard to either an octahedral symmetry or the required magnitudes of the spectroscopic parameters.

4. Conclusion

While this work does pay some attention to experiment, that is not its primary purpose. We merely want to draw attention to the fact that fully symmetry-adapted space/spin wave functions can be constructed and that this leads to considerable simplification of the Hamiltonian matrices. In specific, closed analytical expressions for energies become available and, if limited, even for the effects of configuration interaction. The procedure is general and may be applied to any d^n, f^m ... or mixed electronic configuration. It may become tedious, but it is elegant.

References and Notes

(1) Hipps, K. W.; Crosby, G. A. *Inorg. Chem*. **1974**, *13*, 1543.
(2) Mazur, U.; Hipps, K. W. *J. Phys. Chem*. **1979**, *83*, 1884.
(3) Miskowski, V. M.; Gray, H. B.; Wilson, R. B.; Solomon, E. I. *Inorg. Chem*. **1979**, *18*, 1410.
(4) Mazur, U.; Hipps, K. W. *J. Phys. Chem*. **1980**, *84*, 194.
(5) Eyring, G. T.; Schönherr, T.; Schmidke, H.-H. *Theor. Chim. Acta* **1983**, *64*, 83.
(6) Griffith, J. S. *The Theory of Transition-Metal Ions*; Cambridge University Press: Cambridge, U.K., 1964.
(7) The two symbols ξ and ς do double duty. They identify spin−orbit operator and parameter, respectively, as well as serving as the space orbital identifiers.
(8) Sugano, S.; Tanabe, Y.; Kamimura, H. *Multiplets of Transition-Metal Ions in Crystals*; Academic Press: New York, 1970.
(9) Pierloot, K.; Van Praet, E.; Vanquickenborne, L. G.; Roos, B. O. *J. Phys. Chem.* **1993**, *97*, 12220.